Markov Shape Models: Object Boundary Identification in Serial Magnetic Resonance Images

H. R. Underhill[1], W. S. Kerwin[1]
[1]Radiology, University of Washington, Seattle, Washington, United States

Introduction

Object boundary detection is a fundamental component of automated image analysis. In some medical imaging applications [1,2], confining the search space to a limited shape domain as prescribed by an active shape model (ASM)[3] has been a successful strategy for boundary identification. However, widespread use of the ASM in medical imaging has been restricted since it is susceptible to aberrant results or failure of convergence in regions of the body without distinct edges. To create a more robust method, our proposed technique exploits the three-dimensional data available in magnetic resonance imaging (MRI) by utilizing object descriptors from the previous image to tune the shape algorithm in the next image. Given the similarity to Markov random processes, in which the previous point determines the statistics at the current point in a series, we refer to this approach as a "Markov Shape Model" (MSM). We hypothesized that this technique would greatly reduce the error rate while simultaneously accelerating convergence in automated object boundary detection in serial magnetic resonance images.

Theory

In the general active shape model theory [3], shapes are parameterized by an *nD*-dimensional vector **x** of *n* points along its boundary in *D*-dimensional space. Furthermore, any shape is assumed to be well approximated by $\mathbf{x} \approx \mu_x + b_1\mathbf{p}_1 + b_2\mathbf{p}_2 + \cdots + b_k\mathbf{p}_k$, where μ_x is the mean shape, $\mathbf{p}_k$'s are orthonormal basis functions, b_k's are weights, and $k << nD$. The mean shape of a training set **T** is taken to be μ_x and the $\mathbf{p}_k$'s are the first *k* eigenvectors of the covariance matrix Σ_x of **T**. Within this framework, the object is identified in an unknown image by varying b_k's to enable the deformation of μ_x based on local edge information. The b_k's search space is constrained by $\pm 2\sqrt{\lambda_k}$, where λ_k are the eigenvalues obtained from Σ_x. To create a MSM, we let **y** be a vector containing descriptors from an adjacent image with a mean of μ_y and covariance Σ_y. Assuming **x** and **y** are joint multivariate Gaussian random variables, from conditional model probability theory [4] then $\mu_{\mathbf{x}|\mathbf{y}} = \mu_{\mathbf{x}} + \Sigma_{\mathbf{xy}}\Sigma_{\mathbf{y}}^{-1}(\mathbf{y} - \mu_{\mathbf{y}})$ and $\Sigma_{\mathbf{x}|\mathbf{y}} = \Sigma_{\mathbf{x}} - \Sigma_{\mathbf{xy}}\Sigma_{\mathbf{y}}^{-1}\Sigma_{\mathbf{yx}}$. Thus, given **y**, a "tuned" model can be derived using the conditional mean shape $\mu_{\mathbf{x}|\mathbf{y}}$ and the conditional covariance $\Sigma_{\mathbf{x}|\mathbf{y}}$. If **x** and **y** are correlated, the search space for this model is guaranteed to be smaller. We applied this approach to automated outer-wall boundary identification of the carotid artery near its highly variable bifurcation.

Methods

From a database of high-resolution, axial T1-weighted carotid MRIs, images within 1 cm of the bifurcation from 11 carotid arteries were selected that represented a broad range of possible outer-wall morphology to form **T**. Using the approach described by Cootes et al., a point distribution model was generated for **T**. The vector **y** necessary for the MSM was defined by the width of the shape along a line perpendicular to the major axis at its midpoint from the adjacent more proximal slice, which was manually outlined. Then $\mu_{\mathbf{x}|\mathbf{y}}$ and $\Sigma_{\mathbf{x}|\mathbf{y}}$ were generated for the MSM as previously described. Each model was then iteratively deformed on 16 axial, T1-weighted images from a total of 16 different diseased and non-diseased carotid arteries not included in the training set. Number of iterations until convergence was tabulated and a reviewer blinded to method assessed whether the identified boundary was correct.

Results

The eigenvalues for each of the dominant eigenvectors from the ASM and MSM are listed in Table 1. The search space for the MSM was reduced by 70% compared to the ASM. The mean shape and search space of the first two eigenvectors are illustrated in Fig. 1, where shape information from Fig. 2A is used to refine the search of the MSM for the object in Fig. 2B. Of the 16 test arteries, the ASM correctly identified 7 (43.75%) boundaries and the MSM correctly identified 15 (93.75%). Fig. 2C and 2D contain the mean shape of the ASM and MSM, respectively, prior to their first iterations. Of the 7 cases correctly identified by the ASM, the average number of iterations was 9.7 ± 1.4 (SE). In those same 7 cases, the number of iterations required by the MSM was 5.9 ± 0.9 (SE). In a paired t-test, the MSM required significantly less iteration to converge compared to the ASM ($p < 0.01$).

Table 1. Eigenvalues of the ASM and MSM.

λ_i	ASM Value	MSM Value
λ_1	234	50
λ_2	14	13
λ_3	11	11
λ_4	2	2

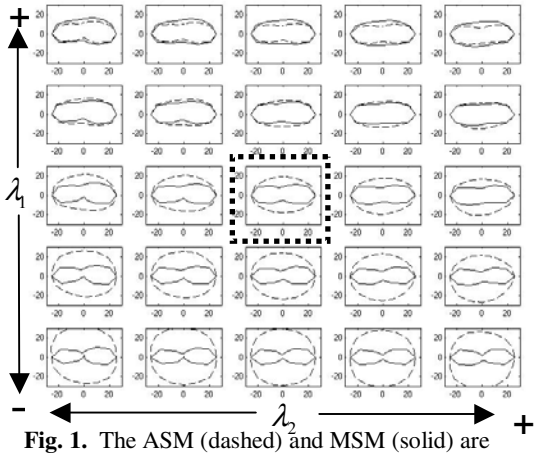

Fig. 1. The ASM (dashed) and MSM (solid) are varied across their first two eigenvectors. The dashed box represents the mean shape for each. Notice the wide search space of the ASM compared to the MSM.

Discussion and Conclusion

The reduced search space of the MSM as displayed in Table 1 afforded a more rapid convergence. Additionally, the closer initialization of the MSM to the desired shape as illustrated in Fig. 2D enabled a significant increase in correct object boundary detection. In MRI, where serial imaging is commonplace, the MSM may be a viable tool for automated object boundary detection.

References

1. Hamarneh et al., Computers in Cardiology, 2000(27): 115-118.
2. Shen et al., NeuroImaging, 2002(15): 422-434.
3. Cootes et al., Comp. Vision and Image Understanding, 1995(61): 38-59.
4. Leon-Garcia, Probability and Random Processes for Electrical Engineers, Addison-Wesley 1989.

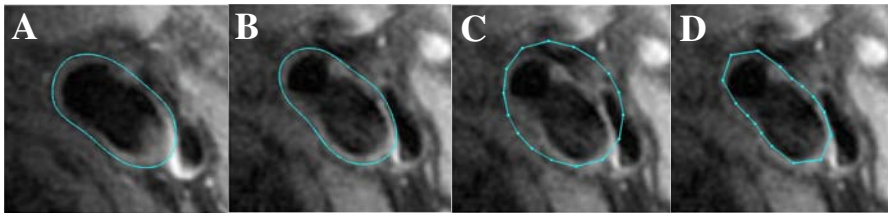

Fig. 2. Image A is the shape proximal to the carotid bifurcation (B). Image C and D are the initial shapes of the ASM and MSM, respectively. The ASM failed to identify the correct boundary, while the MSM converged correctly.